J|A|C|S
ARTICLES
Published on Web 06/27/2006

# Columnar Self-Assembled Ureido Crown Ethers: An Example of Ion-Channel Organization in Lipid Bilayers

Adinela Cazacu,[†] Christine Tong,[‡] Arie van der Lee,[†] Thomas M. Fyles,*[,‡] and Mihail Barboiu*[,†]

*Contribution from the Institut Européen des Membranes - UMR−CNRS 5635, Place Eugène Bataillon, CC 047, F-34095 Montpellier, Cedex 5, France, and Department of Chemistry, University of Victoria, Victoria, BC, V8W3V6, Canada*

Received March 25, 2006; E-mail: mihai.barboiu@iemm.univ-montp2.fr; tmf@uvic.ca

***Abstract:*** The self-assembly of ureido crown-ether derivatives has been examined in homogeneous solution, in the solid state, and in planar bilayer membranes. The self-assembly is driven by head-to-tail hydrogen bonding between the urea functional groups. Dimers and higher oligomers are formed in $CDCl_3$ solution as assessed by the change in the ureido NH chemical shift as a function of concentration. Single-crystal X-ray diffraction shows that an antiparallel association of the ureas produces columnar channels composed of face-to-face crown ethers. Powder X-ray diffraction studies also show the presence of a minor phase based upon a parallel urea association leading to an alternative columnar arrangement of the crown ethers. In bilayer membranes at low concentration of ureido crown ether added, membrane disruption is observed together with rare single-channel openings, but at higher concentration, a rich array of interconverting channel conductance states is observed. The channel results are interpreted as arising from discreet stacks of ureido crown ethers where the transport of cations would occur via the macrocycles, admixed with larger pores formed by association of the crown ether headgroups around a central large pore.

## Introduction

Numerous artificial membrane transport systems utilizing carriers or channel-forming structures have been developed in the past decades.[1,2] Crown ethers,[3] cyclic peptides,[4] oligophenyl barrel-stave structures,[5] and oligoester bola-amphiphiles[6] have all been used in this context. Concurrently, the design and application of new heteroditopic receptors capable of simultaneous coordination of both cations and anions have attracted a great deal of interest as these systems have many potential functions, such as solubilization, extraction, and membrane transport.[7] Convergent multidimensional self-assembly strategies have been used for the synthesis of noncovalent self-organized devices, designed to mimic natural ion-channel proteins. Despite their thermodynamic stability, such structures are in dynamic equilibrium between monomer and supramolecular oligomers, and only a few examples clearly showed single-channel activity in lipid bilayers.[8]

We are interested in the possibility to self-organize receptors containing suitable molecular instructions for recognition- and membrane transport-based functions. We have recently reported the first examples of this type of synthetic system on the basis of the neutral heteroditopic ureido crown ether **1.** This compound can complex both anions and cations and can self-organize in solution and in the solid state into tubular ribbon superstructures (Figure 1).[7a] These self-organization properties in a liquid membrane phase provided the first evidence for a possible hybrid transport process combining carrier and channel mechanisms in correlation with the self-assembly properties of these heteroditopic receptors.[7b] Furthermore these dynamic self-organized systems have been "frozen" in a polymeric hybrid matrix by a sol−gel process, opening the door to the design of a novel class of solid hybrid membranes.[7h]

[†] Institut Européen des Membranes.
[‡] Department of Chemistry, University of Victoria.

(1) (a) Hucho, F.; Weise, C. *Angew. Chem., Int. Ed.* **2001**, *40*, 3100−3116. (b) Gouaux, E.; MacKinnon, R. *Science* **2005**, *310*, 1461−1465.
(2) (a) Lehn, J.-M. *Supramolecular Chemistry − Concepts and Perspectives*; VCH: Weinheim, 1995; Chapter 6. (b) Matile, S.; Som, A.; Sorde, N. *Tetrahedron* **2004**, *60*, 6405−6435. (c) Koert, U.; Al-Momani, L.; Pfeifer, J. R. *Synthesis* **2004**, 1129−1146. (d) Boon, J. M.; Smith, B. D. *Curr. Op. Chem. Biol.* **2002**, *6*, 749−756.
(3) (a) Gokel, G. W.; Mukhopadhyay, A. *Chem. Soc Rev.* **2001**, *30*, 274−286. (b) Voyer, N. *Top. Curr. Chem.*; Springer-Verlag: Berlin, Heidelberg, 1996; p 1−35.
(4) Bong, D. T.; Clark, T. D.; Granja, J. R.; Ghadiri, M. R. *Angew. Chem., Int. Ed.* **2001**, *40*, 988−1011.
(5) (a) Matile, S. *Chem. Soc. Rev.* **2001**, *30*, 158−167. (b) Sakai, N.; Mareda, J.; Matile, S. *Acc. Chem. Res.* **2005**, *38*, 79−87.
(6) (a) Eggers, P. K.; Fyles, T. M.; Mitchell, K. D. D.; Sutherland, T. *J. Org. Chem.* **2003**, *68*, 1050−1058. (b) Fyles, T. M.; Hu, C.; Knoy, R. *Org. Lett.* **2001**, *3*, 1335−1337. (c) Fyles, T. M.; Loock, D.; Zhou, X. *J. Am. Chem. Soc.* **1998**, *120*, 2997−3003. (d) Fyles, T. M.; Kaye, K. C.; Pryhitka, A.; Tweddel, J.; Zojaji, M. *Supramol. Chem.* **1994**, *3*, 197−209.
(7) (a) Barboiu, M.; Vaughan, G.; van der Lee, A. *Org. Lett.* **2003**, *5*, 3073−3076. (b) Barboiu, M. *J. Incl. Phenom. Mol. Rec.* **2004**, *49*, 133−137. (c) Koulov, A. V., Mohoney, J. M.; Smith, B. S. *Org. Biomol. Chem.* **2003**, *1*, 27−29. (d) Gale, P. A. *Chem. Commun.* **2005**, 3761−3772 and references therein. (e) Custelecean, R.; Delmau, L. H.; Moyer, B. M.; Sessler, J. L.; Cho, W.-S.; Gross, D.; Bates, G. W.; Brooks, S. J.; Light, M. E.; Gale, P. *Angew. Chem., Int. Ed.* **2005**, *44*, 2537−2542. (f) Gong, J.; Gibb, B. C. *Chem. Commun.*, **2005**, 1393−1395. (g) Lankshear, M. D.; Cowley, A. R.; Beer, P. D. *Chem. Commun.* **2006**, 612−614 (h) Barboiu, M.; Cerneaux, S.; Vaughan, G.; van der Lee, A. *J. Am. Chem. Soc.* **2004**, *126*, 3545−3550.
(8) Ghadiri, M. R., Granja, J. R.; Buehler, L. K. *Nature* **1994**, 369, 301−304; Kaucher M. S.; Harrell, W. A.; Davis, J. T. *J. Am. Chem. Soc.* **2006**, *128*, 38−39.

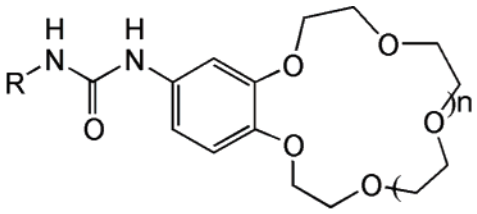

**1**, n=1, R= -$C_6H_5$; **2**, n=1, R= -$C_3H_7$; **3**, n=1, R= -$C_6H_{13}$, **4**, n=1, R=-$C_{18}H_{37}$
**5**, n=2, R= -$C_3H_7$; **6**, n=2, R= -$C_6H_{13}$, **7**, n=2, R=-$C_{18}H_{37}$

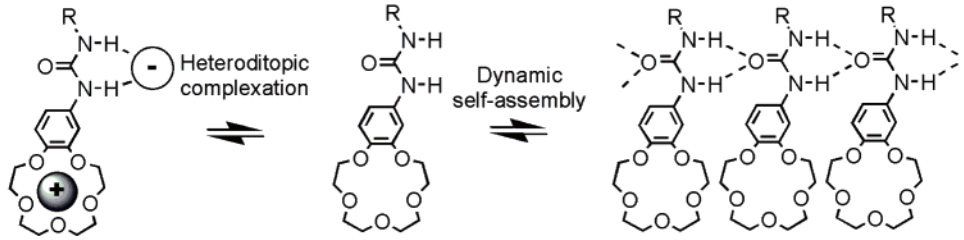


***Figure 1.*** Dynamic self-organization in solution and in the solid state of the heteroditopic receptors **2**−**7**.

From the mechanistic point of view, we start with monomers that are carrierlike transporters and allow them to self-assemble into oligomeric crown-ether supramolecular aggregates. The superstructures produced are potentially membrane-spanning channel-like transporters (Figure 1). We therefore decided to synthesize and to study an extended series of new hydrogen-bonded alkylurea-crown ethers **2**−**7** for their ability to form aggregates in the solution phase, channel-like arrays in the solid state, and functional ion channels in planar bilayer membranes. This system therefore illustrates the convergence of supramolecular self-organization and supramolecular function.

## Results and Discussion

**Synthesis of Receptors 2−7.** Six (ureido)crown-ether receptors **2**−**7** were prepared for the studies described here. We restricted our studies to benzo15-crown-5 and benzo18-crown-6 as selective macrocyclic derivatives and to propyl **2**, **5**, hexyl **3**, **6**, and octadecyl, **4**, **7** as alkyl termini of different lengths and lipophilicity. The alkylisocyanate was treated with the corresponding aromatic aminobenzocrown ether ($CH_3CN$, Δ, 5h) to afford, after crystallization, **2**−**7** as white powders (90%). The $^1H$, $^{13}C$ NMR, ESI-MS spectra are in agreement with the proposed formula.

**Solution Self-Assembly Studies of Receptors 2−4.** $^1H$ NMR dilution experiments conducted on $CDCl_3$ solutions of **2**−**4** showed a strong downfield shift of NH protons upon increasing concentration, which is indicative of self-association through intermolecular hydrogen bonding (Figure 2).

Equilibration between hydrogen-bonded and non-hydrogen bonded states in $CDCl_3$ for a given N−H proton is almost always fast on the NMR time scale and observed proton chemical shifts are weighted averages of the chemical shifts of contributing states. The downfield proton chemical shifts are a complex function of the concentration, showing at least three step increases to two plateaus. This is suggestive of stepwise association processes to form at least two distinct types of aggregates. We assume that the process occurring at the lowest concentrations is the formation of a dimer from monomers.

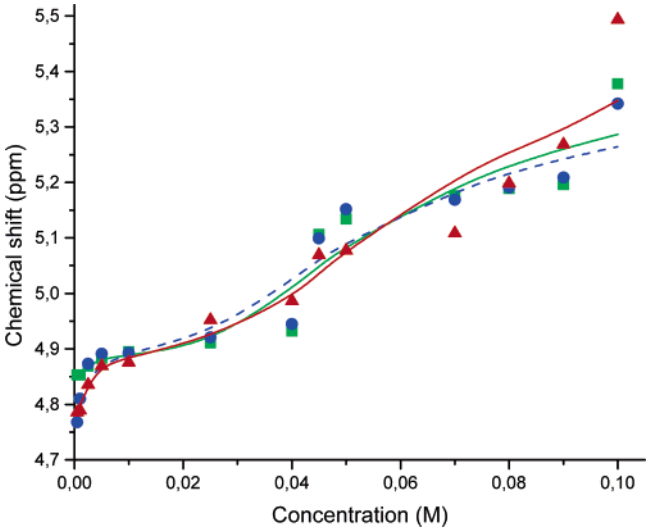


***Figure 2.*** Chemical shifts of the Alkyl-N−H proton plotted against total concentration of **2** (red triangles), **3** (blue circles), and **4** (green squares) in $CDCl_3$ at 25 °C. Lines are calculated using the model described in the text.

In this view, the dimer would be essentially fully formed below 0.01 M, but it is not until at least four times higher concentration that the second type of species emerges. This unusual behavior is not consistent with the formation of a range of simple oligomers beyond the dimer, such as a trimer or a tetramer (dimer of dimers), because these species would give a steady change over the concentration range. Rather, the second plateau indicates the formation of stable oligomeric species of a defined stoichiometry. There is clearly a third process at high concentration, but the data do not extend to a third plateau (if there is one). Consequently, there has been no attempt to model the third step. The first two steps can be analyzed by considering the following equilibria:

(1) 2M ↔ D; where M is the monomer and D is the dimer

(2) $n$M ↔ $M_n$; where $M_n$ is an aggregate of defined stoichiometry $n$.

The formation constant for step (1) is:

(3) $K_d = [D]/[M]^2$

***Table 1.*** Association Constants and Chemical Shifts for Numerical Fits to a Monomer/Dimer/Defined Aggregate Model

| | **2** | **3** | **4** |
|---|---|---|---|
| $K_d$ ($M^{-1}$) | $175 \pm 24$ | $130 \pm 8$ | $150 \pm 60$ |
| $K_S$ ($M^{-1}$) | $70 \pm 7$ | $65 \pm 5$ | $70 \pm 16$ |
| $\delta_M$ (ppm) | $4.75 \pm 0.07$ | $4.78 \pm 0.05$ | $4.84 \pm 0.06$ |
| $\delta_D$ (ppm) | $4.98 \pm 0.10$ | $4.99 \pm 0.09$ | $4.93 \pm 0.11$ |
| $\delta_n$ (ppm) | $5.69 \pm 0.23$ | $5.50 \pm 0.12$ | $5.57 \pm 0.13$ |
| $n$ | $17 \pm 2$ | $17 \pm 7$ | $16 \pm 8$ |
| $r^2$ | 0.9998 | 0.9999 | 0.9999 |
| cod | 0.9171 | 0.9438 | 0.9278 |

and the formation constant for step (2) is:

(4) $K_n = [M_n]/[M]^n$

The data can be fit using this model using three chemical shifts (monomer, dimer, oligomer), two formation constants ($K_d$, $K_n$), and the aggregate stoichiometry ($n$) as unknowns. Numerically, this is not very robust as the value of $K_n$ is very large ($>10^{20}$) whereas $K_d$ is only of the order of $10^2$. We therefore assume an average stepwise binding constant ($K_S$) such that:

(5) $K_n = (K_S)^n$

The assumption of eq 5 is equivalent to assuming that every monomer binds to any aggregate of any size with the same affinity. This model is numerically more robust and gives reasonable fits to the data, as shown in Figure 2. The values of the constants determined are given in Table 1. There is encouraging similarity in the constants derived from the fit as there should be, but the precision of some of the values is modest. This is a direct result of the limitations of the model as seen from two different measures of the overall statistical validity of the fit. The $r^2$-values are uniformly high, indicating that there is a good minimum around each value. However, the coefficient of determination (cod) is not as good, indicating that the model itself is not correct in some respect. In other words, the data are consistent with the model described, but the model is too simplistic. The model assumes only one aggregate species forms. This is unlikely, and a collection of species with a range of stoichiometries is more likely. However, even this rather simple model will clearly reproduce the successive stages of association evident in the data. The first association occurs with the expected value for a hydrogen bonding interaction in a noncompeting solvent. The second interaction is apparently weaker on a stepwise basis, possibly as a result of some steric inhibition to the formation of the structure.

**Solid-State Structure of Receptor 6.** Additional information concerning receptor self-organization and binding behavior is obtained from the single-crystal structure of **6** and the X-ray powder diffraction of compounds **2**−**7**. Crystals suitable for X-ray structure determination were obtained by slow evaporation of an acetonitrile solution of **6** on a glass slide at room temperature. The molecular structure and packing are presented in Figure 3. The structure of **6** reveals the expected urea macrocycle. The unit cell contains four ureido-benzocrown-ether molecules. The urea moiety and the phenyl ring are disposed in an angular position (45.8°) with respect to the plane of the macrocycle. The relative arrangement of the crown-ether molecules in the crystal is different from previously reported ureido-benzocrown-ether-type superstructures[7a,h] and deserves some comment. The H−O distances of 2.04 and 2.08 Å alternate along the urea ribbon and are consistent with other urea systems.[9] Two neighboring urea planes are disposed at an angle of about 123° with respect to one another, imposing a zigzag conformation on the urea-ribbon that is very different from the planar conformation observed in the crystal structure of the benzo(ureido)crown-ether **1**.

As shown in Figure 3a, and despite the uniformity of the urea H-bond distances over the whole urea-ribbon, the molecules of **6** are organized as dimers. Two individual molecules are stacked in an antiparallel dimeric aggregate, presenting a tight contact between the hexyl substituents and the neighboring benzocrown moieties. The dimers interact by weak van der Waals interactions such that each hexyl group is asymmetrically sandwiched between two benzocrown-ether groups. One of these comes from one dimer (centroid−centroid distances of 3.83, 3.91, and 4.01 Å), and the other one comes from a neighboring dimer (centroid−centroid distances of 4.71, 4.75, and 4.26 Å), Figure 3b.

Accordingly columnar arrays of channel-type stacks of crown ethers are generated in the solid state by the self-organization process, such that the crown ether moieties are disposed in an antiparallel arrangement with an average crown centroid−crown centroid distance of 8.23 Å.

The ureido-benzocrownethers **2**−**7** were investigated by X-ray powder diffraction (Figure 4). For compound **6**, it was possible to obtain full atomic structure determination and to generate the corresponding diffractogram using the data of single-crystal measurements. Comparing the diffractogram generated from the single-crystal structure solution (Figure 4, green) with the experimental diffraction results of the bulk powder of **6** (Figure 4, red), shows that preferential antiparallel dimeric packing coexists with a second residual polymorph. It can be postulated that in the solid state the *antiparallel packing* corresponding to the first intense peak is preferential to the residual *parallel packing* corresponding to the second small peak (Figure 5). The first intense diffraction peaks corresponding to the (100) reflections are related to the distance *a* of the elementary cell (Figure 6a). Over the suite of compounds, the *a* distances are in perfect correlation with the length of the molecule (Figure 6b) obtained by molecular modeling of the structures of these complexes on the basis of the geometry of **1**[7a] and **6** in the crystal structure, using a linear geometry for the alkyl ($C_3H_7$-, $C_6H_{13}$- $C_{18}H_{37}$-) substituents.

We can assume that the main three-dimensional organization of **5** and **7** is approximately equal to that of **6**, i.e., a similar geometrical disposition relative to the plane *ac* of the macrocycles, leading to the formation of two dimers in the elementary cell. The elementary unit cell (i.e., dimension *a*) clearly increases, because the first primary peak shifts to the right when going from **5** to **7** and the increase is proportional to the length of the molecule (alkyl substituent). We assume that propagation of the macrocycles along the main direction *b* results in the formation of oligomers of dimers of **5**−**7**, like those observed for the compound **6**.

**Membrane Activity.** Compounds **2**−**7** were surveyed for their ability to form single channels in planar bilayer membranes using a range of alkali cation electrolytes. We have previously done such a survey in which we defined general classes of activity in an attempt to distinguish reproducible conductance changes (channels), from random events (disruption).[12] The same approach was used in this survey: aliquots (5 $\mu$L) of a

(9) Etter, M. C. *Acc. Chem. Res.* **1990**, *23*, 120−126.

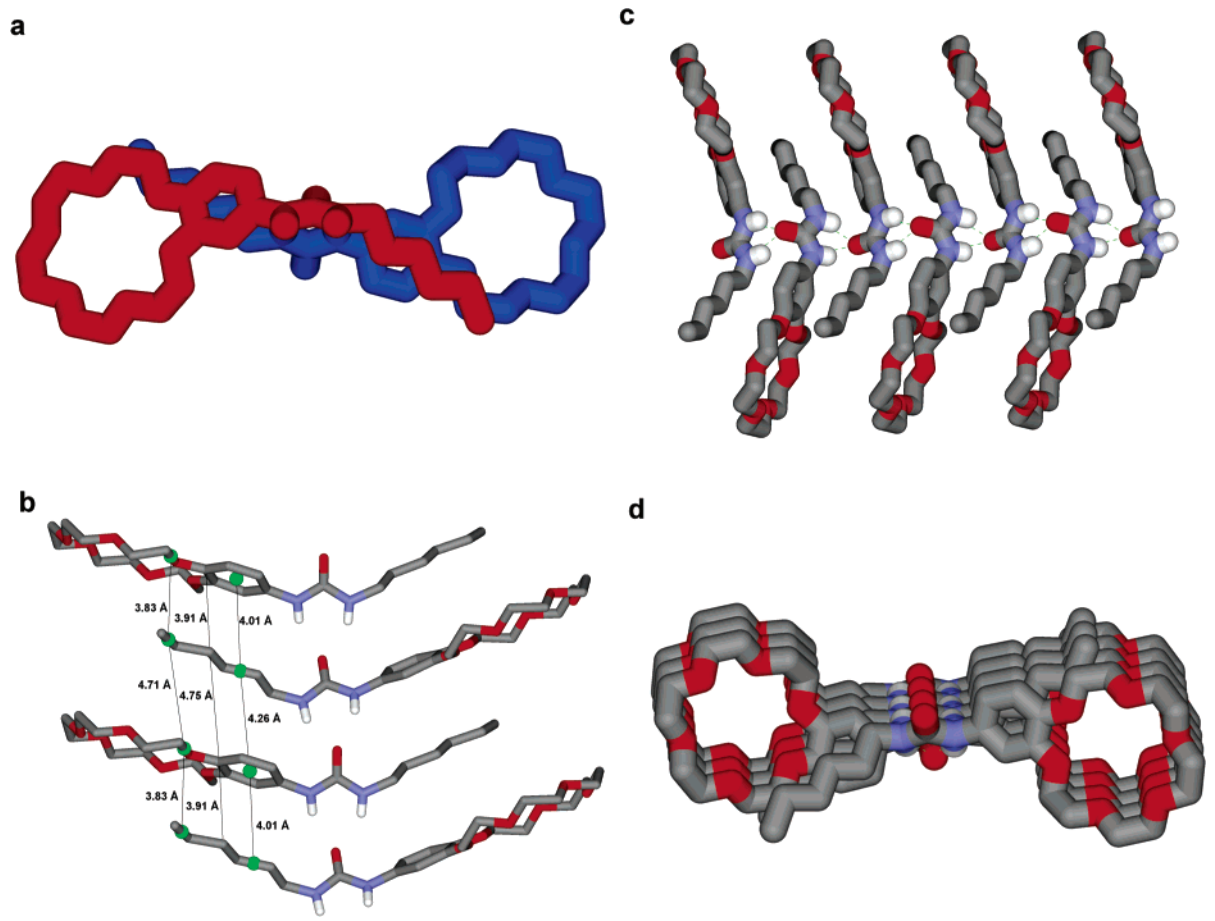


***Figure 3.*** Crystal structure of macrocyclic receptor **6** stick representation of (a) a single dimer, (b) dimer packing distances, (c) and (d) two side views of the crystal packing of **6** in the H-bond channel-type superstructures.

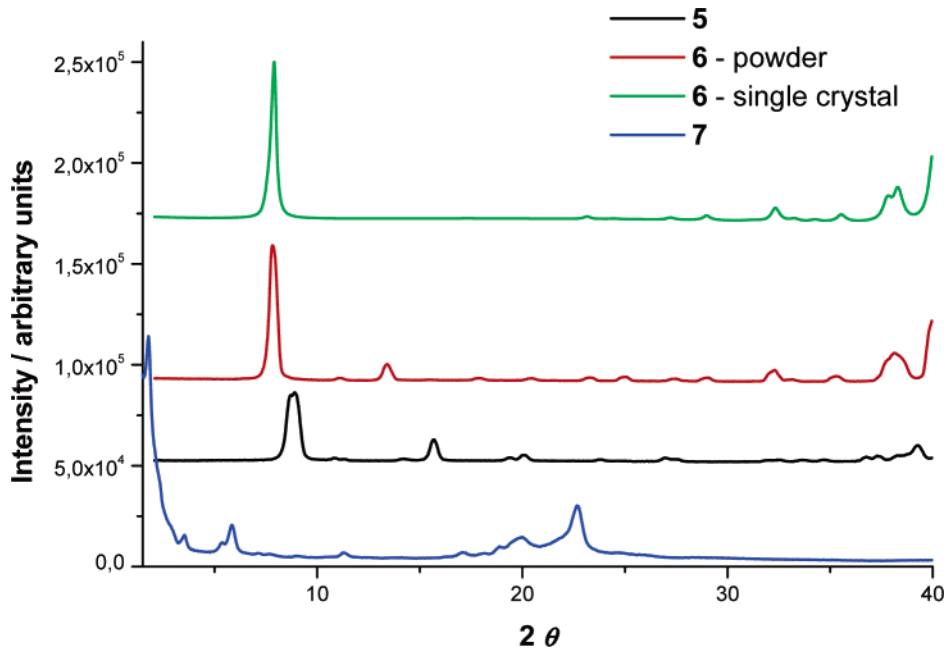


***Figure 4.*** X-ray powder diffraction pattern of the ureidobenzo18-crown-6 compounds **5**−**7** and single-crystal pattern of **6** (green).

methanol (**2**, **3**, **5**, **6**) or DMSO (**4**, **7**) solution (0.2−0.3 mM) were injected into a two-compartment cell in which a stable bilayer membrane had been formed. All six compounds elicited a level of membrane disruption activity within a few minutes of exposure to the small amount of compound added. During "membrane disruption," the majority of openings are spikes of very short duration and highly variable amplitude. The late section of Figure 7B is typical of this type of activity. At the early times in Figure 7B, there appear to be some square-top openings of relatively long duration with spikes superimposed.

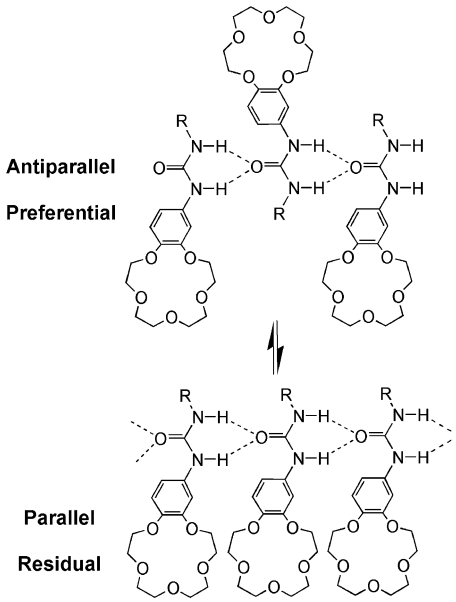


***Figure 5.*** Antiparallel and parallel dynamic self-organization of H-bonded urea oligomers.

It proved to be extremely difficult to observe square-topped openings without competing membrane disruption activity; the remaining sections of Figure 7 (A,C,D) show 3 of about 10 examples recorded during 20 separate experiments of 1−2 h duration each. Only compound **3** showed the square-top openings at these initial low concentrations.

On the basis of the two-stage behavior discussed for the solution aggregation experiments (Figure 2), we explored conditions in which substantially more compound was introduced to the membrane. This was accomplished by injection of aliquots of a 10-fold more concentrated stock solution or through direct mixing of ureido-crown ethers with lipid prior to membrane formation. Significant membrane disruption was observed in a large majority of cases, but compound **6** showed complex, but clearly regular, channel behavior as illustrated in Figure 8. Although the 15-crown-5 derivative **3** gave some evidence of regular channel activity at low concentration (Figure 7), there was no evidence of any regular behavior at the higher concentration. Compound **6** showed rare square-top channel behavior akin to Figure 7 at low concentration but abundant activity at the higher concentration of Figure 8. These differences preclude any direct comparison of the effect of the crown ether ring size on the channel formed.

The puzzling feature of the observations in Figure 8 is the extremely wide range of conductance levels observed, both in terms of the durations of the openings (milliseconds to seconds) and the magnitude of the currents (10−200 pA). The expanded section on the right of Figure 8 shows that within each trace, there are clear sections of steplike behavior. Over a number of experiments, it appeared that there are channels that carry about 20 pA current that have two relatively closely spaced levels

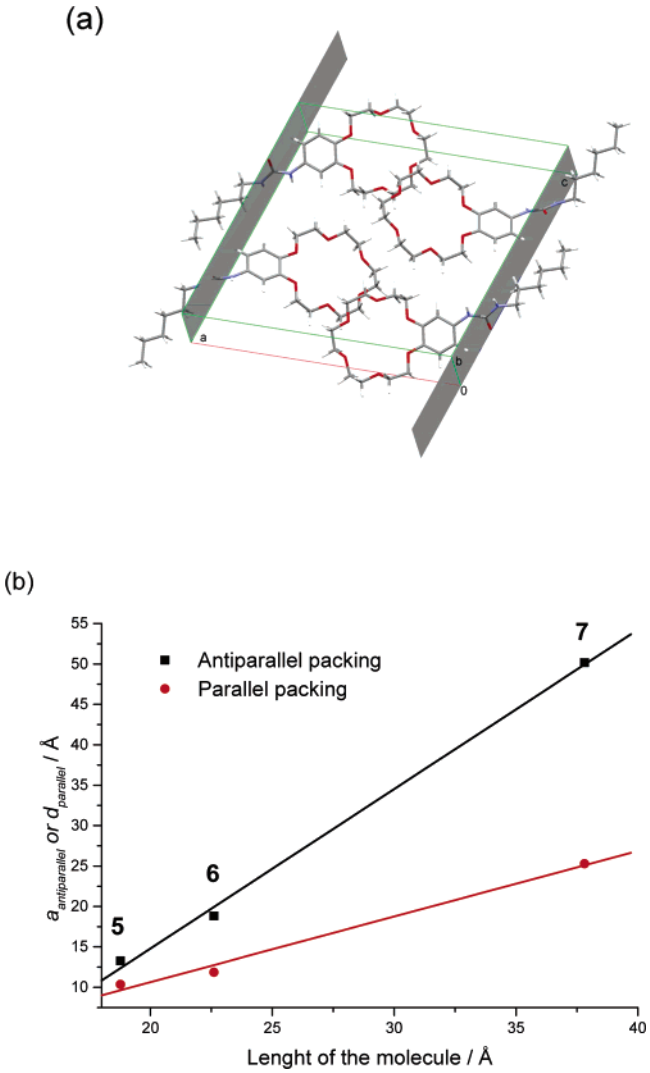


***Figure 6.*** (a) Elementary unit cell and (b) the corresponding distances of the antiparallel and of the parallel packing distances calculated from powder diffractions patterns plotted against the molecular length of **5**−**7**.

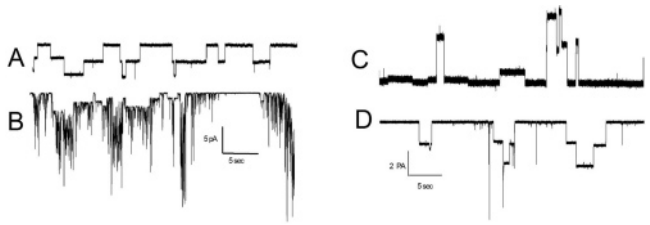


***Figure 7.*** Membrane activity shown by **3** in a diPhyPC membrane with 1 M $KNO_3$ electrolyte. (A,B) −100 mV applied potential; (C,D) −140 mV applied potential.

(top trace in Figure 8B). At the other extreme there are long-lived channels that can carry very large currents (bottom trace of Figure 8A). In an intermediate region, there are short duration channels that "bridge" the two ranges with a number of levels (middle trace in Figure 8B).

The analysis of this complex behavior is illustrated with respect to the data trace in Figure 9. The data file (40 s duration) was sorted into a histogram of the number of occurrences of a particular current and a smooth curve was fit to the overall histogram. This overall curve was then fit to the sum of a series of Gaussians as illustrated in Figure 9 (left) to give four levels,

(10) (a) Voyer, N.; Meillon, J.-C. *Angew. Chem., Int. Ed. Engl.* **1997**, *36*, 967−968. (b) Vandenbourg, Y.-R.; Smith, B. D.; Biron, E.; Voyer, N. *Chem. Commun.* **2002**, 1694−1695. (c) Winum J.-Y.; Mantile S. *J. Am. Chem. Soc.* **1999**, *121*, 7961−7962; (d) Otis, F.; Voyer, N.; Polidori, A.; Pucci, B. *New J. Chem.* **2006**, *30*, 185−190.
(11) Yang, L.; Harroun, T. A.; Weiss, T. M.; Ding, L.; Huang, H. W. *Biophys J.* **2001**, *81*, 1475−1485.
(12) Fyles, T. M.; Knoy, R.; Müllen, K.; Sieffert, M. *Langmuir* **2001**, *17*, 6669−6674.

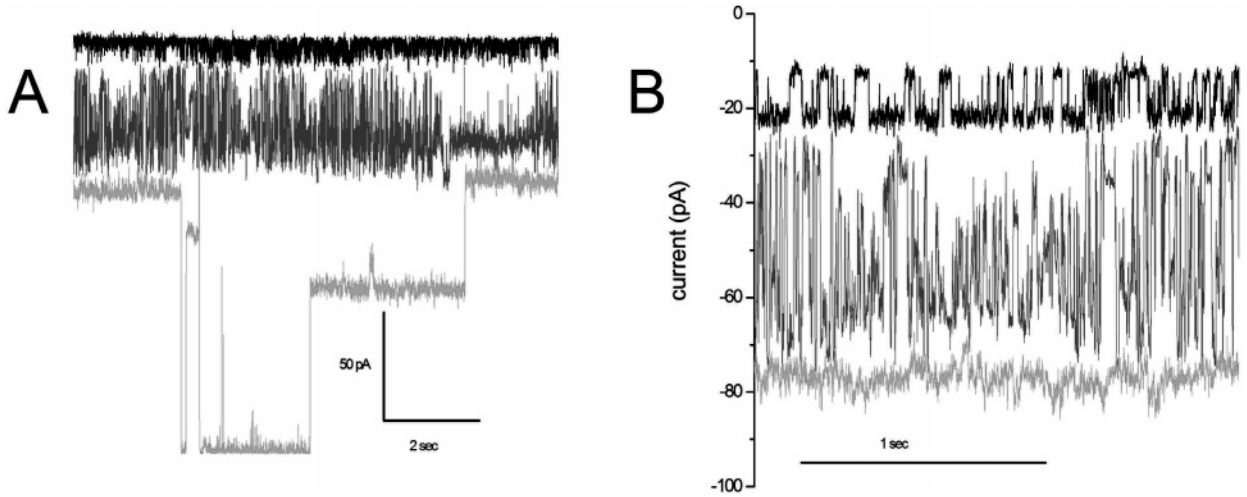


***Figure 8.*** Membrane activity of **6** at high concentration in a diPhyPC membrane with 1 M $KNO_3$ electrolyte at −130 mV applied potential. (A) Long duration view of several different experiments; (B) close up showing levels from separate experiments.

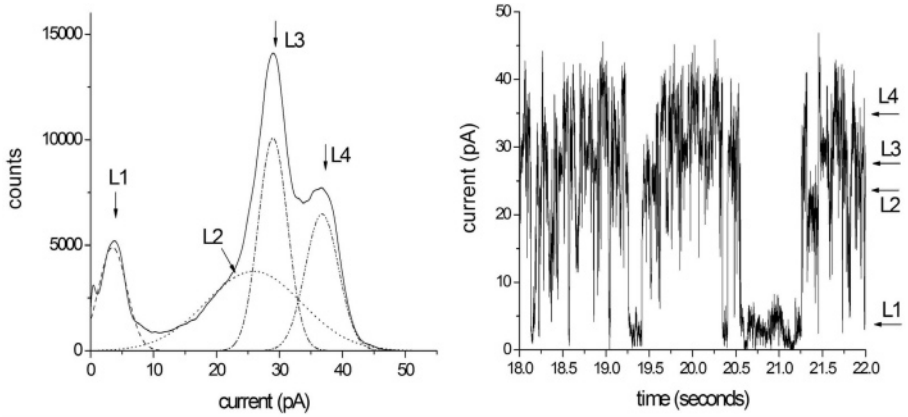


***Figure 9.*** (Left) Smoothed all points histogram for a 40 s file with a bin size of 0.5 pA together with fitted Gaussians; (Right) short portion of the raw data trace showing regions in the data with the Gaussians identified overlapped (**6**; diPhyPC, 1 M $KNO_3$, −90 mV).

which account for the overall file. These levels can be seen in a short section of the original data as illustrated on the right of Figure 9.

With the individual data files analyzed as above, the observed values of the peak currents were converted to conductance values and sorted to align levels from different data files having the same conductance within the width of the fitted Gaussian. The levels were assigned a "label" centered at zero such that levels with the same absolute value of the conductance have the same assigned level. For example level "−5" with a conductance of −142 pS was equated with level "5" with a conductance of +142 pS. As a check during the assignment, the iV curves for the assigned levels were continually examined. The expectation for large conductance channels is that they will obey Ohm's law; thus, a linear relationship crossing zero is expected. This expectation is fulfilled up to about level ±7, but there were too few examples to allow this check above that conductance level. Finally, the conductance was plotted as a function of level label to generate the curve in Figure 10. The label assignments are not very secure above ±7, particularly for positive conductance. To the extent that there are more negative conductance levels observed, this part of the curve is more reliable.

The conductance behavior of this system is novel. Usually, channel forming compounds give only a few levels, and when

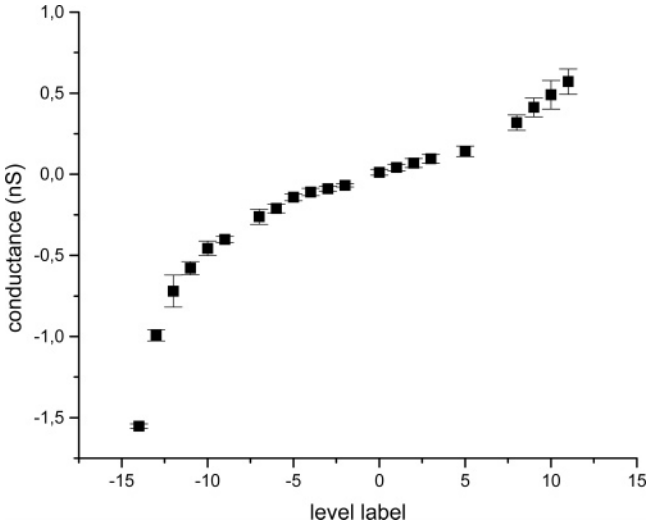


***Figure 10.*** Conductance as a function of level label.

many levels do occur, they become less likely and more similar as the conductance increases.[6] The lifetime of individual levels is usually comparable. In contrast, the very large conductance channels made by **6** are the longest lived, and it is the intermediate cases that are the short-lived and poorly defined ones. The lower conductance levels, near the middle of the

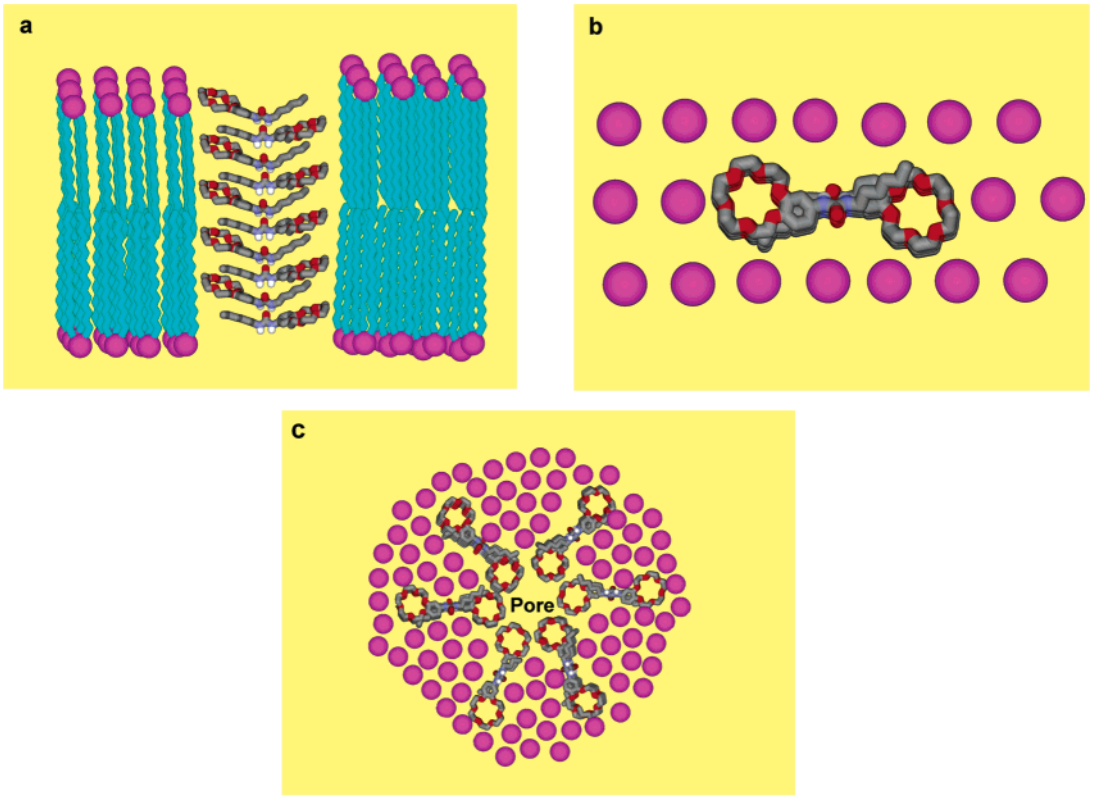


***Figure 11.*** Schematics of the double barreled model (a) lateral and (b) top view and (c) the possible organization of components in a toroidal model.

range, are again longer lived and show discrete levels and transitions. One possibility is that there are two types of structures: one to give the center part of the Figure 10 curve, and the other to account for the high conductance/long-lived channels at the extremes.

Conductance is related to pore diameter and pore length through the Hille equation.[13] If we take 0.15 nm as the radius of an 18-crown-6, and a channel length of 3−3.5 nm equivalent to the thickness of a bilayer membrane, then the conductance of a single channel of crown ethers would be expected to be 27−31 pS. This is approximately the slope per level in the center region of Figure 10 (29.5 ± 0.9 pS/level for levels −5 to 5). The channels in this region could be viewed as derived from a section of the crystal structure of **6** in which five dimers would form a double-barreled channel as illustrated in Figure 11a,b. The loss of one crown ether from this stack would shorten the channel and would lead to a higher conductance state. The multiple levels observed for these species would then be interpreted as multiple copies of these double-barreled channels each of which is gaining and loosing the outermost crown ethers to account for the central portion of Figure 10. Part of the complexity in this region is due to the requirement of a high concentration to produce the stacks, which will also lead to multiple copies of these species in this concentration range.

The high conductance channels must have some other structure. If we assume that the largest conductances involve a structure about the thickness of a bilayer (3−4 nm), then a radius of 0.5 nm is required. This is much too large for a single crown ether. One possibility is that the crown ether acts as a neutral surfactant to stabilize a toroidal pore similar in structure to those proposed by Colombini[14] for the pores formed by ceramide. The walls of the pore would be lined with crown ethers with the alkyl tails projecting into the lipid hydrocarbon region. The relatively large size of the polar headgroup relative to the hydrocarbon tail would stabilize the positive curvature required on the inside of the torus. One possible top view of these larger pores are sketched in Figure 11 c.

## Conclusions

This is a very intriguing system. In homogeneous solution, at least two types of hydrogen bonded aggregates form, which can be modeled as a dimer followed by a discrete higher oligomer, perhaps as large as a hexadecamer. In the solid state, a dominant antiparallel ribbon of urea self-association leads to extended stacks of crown ethers. A minor polymorph consisting of the previously observed parallel urea ribbons is also observed. Finally, in a bilayer membrane system, the compounds form channels reluctantly at low concentration, preferring to give disruption over regular behavior. At higher concentration where channels do form, there are apparently two types of structures formed. They show a basic regularity, suggesting structural constraints, but they show an immense range of conductance values and lifetimes.

It is very tempting to equate the two types of hydrogen-bonded structures in the solid state (parallel and antiparallel), with the two types of aggregates in solution (dimer and high oligomer), and with the two types of channels in the bilayer membrane (possible stacked crown ethers and a large toroidal

(13) Hille, B. *Ionic Channels of Excitable Membranes*, 2nd ed.; Sinauer Associates, Incorporated: Sunderland, 1992; p 383.

(14) (a) Siskind, L. J.; Davvoody, A.; Lewin, N.; Marshall, S.; Colombini, M.; *Biophys J.* **2003**, *85*, 1560−1575. (b) Yang, L.; Haroon, T. A.; Weiss, T. M.; Ding, L.; Huang, H. W. *Biophys J.* **2001**, *85*, 1475−1485.

pore). The unifying assumption is that an antiparallel dimer would form preferentially. Stacks of these dimers would lead to the dominant solid-state structure and, in a membrane environment, to a double-barreled channel as illustrated in Figure 11. The parallel dimer and oligomer would place the alkyl groups on the same face of the structure, in a fashion that could stabilize the large pores observed.

The above results describe a simple synthetic supramolecular self-organized system that successfully combines both supramolecular structure and supramolecular function. Ion channels based on covalently bound crown-ethers[3,10,15] have been known for a considerable time. More recently, organized assemblies of crown ether stacks within liquid crystalline phases[16,17] have created directional conduction pathways in solid materials illustrating another type of ion-channeling at the molecular and the supramolecular level. The system we describe here is the first example of a supramolecular device where the structural and functional aspects of supramolecular self-organization might, in principle, be associated.

**Acknowledgment.** A.C. thanks the CROUS Montpellier for a doctoral fellowship. We thank Dr. Gavin Vaughan (ID11, ESRF, Grenoble France) for the single-crystal X-ray measurements This research was supported in part by the European Science Foundation (ESF), and European Heads of Research Councils (EUROHORCs), EURYI Award 2004 (M.B.), by the CNRS, and by the Natural Sciences an Engineering Research Council of Canada.

**Supporting Information Available:** Experimental procedures and full characterization for compounds **2**−**7**. Crystallographic data for **6**. This materials is available free of charge via the Internet at http://pubs.acs.org.

JA061861W

(15) (a) Neevel, J. G.; Nolte, R. J. M. *Tetrahedron Lett.* **1984**, *25*, 2263−2266. (b) Nolte, R. J. M.; van Beijnen, A. J. M.; Neevel, J. G.; Zwikker, J. W.; Verkley, A. J.; Drenth, W. *Isr. J. Chem.* **1984**, *24*, 297−301. (c) Kragten, U. F.; Roks, M. F. M.; Nolte, R. J. M. *Chem. Commun.* **1985**, 1275−1276.

(16) (a) Percec, V.; Bera, T. K. *Tetrahedron* **2002**, *58*, 4031−4040. (b) Percec, V.; Bera, T. K. *Biomacromolecules* **2002**, *3*, 167−181.

(17) (a) Huang, Z. B.; Kang, T. J.; Chang, S. H. *New J. Chem.* **2005**, *29*, 1616−1620. (b) Gromov, S. P.; Vedernikov, A. I.; Ushakov, E. N.; Lobova, N. A.; Botsmanova, A. A.; Kuzmina, L. G.; Churakow, A. V.; Strelenco, Y. A.; Alfimov, M. V.; Howard, J. A.; Johnels, D.; Edlund, U. G. *New J. Chem.*, **2005**, *29*, 881−894. (c) Begin, U.; Zipp, G.; Möller, M. *Adv. Mater.* **2000**, *12*, 510−513. (d) Steike N.; Frey, W.; Baro A.; Laschat, S.; Dress, C.; Nimtz, M.; Hagele, C.; Giesselman, F. *Chem.*−*Eur. J*, **2006**, *12*, 1026−1035.